Separation Science and Technology
Publication details, including instructions for authors and subscription information:
http://www.informaworld.com/smpp/title~content=t713708471

MINOR ACTINIDE PARTITIONING BY LIQUID-LIQUID EXTRACTION: USING A SYNERGISTIC MIXTURE OF BIS(CHLOROPHENYL)-DITHIOPHOSPHINIC ACID AND TOPO IN A HOLLOW FIBER MODULE FOR AMERICIUM(II)-LANTHANIDES(III) SEPARATION

Andreas Geist[a]; Michael Weigl[a]; Klaus Gompper[a]
[a] Forschungszentrum Karlsruhe GmbH, Institut für Nukleare Entsorgung, Karlsruhe, Germany

Online publication date: 23 October 2002

To cite this Article Geist, Andreas , Weigl, Michael and Gompper, Klaus(2002) 'MINOR ACTINIDE PARTITIONING BY LIQUID-LIQUID EXTRACTION: USING A SYNERGISTIC MIXTURE OF BIS(CHLOROPHENYL)-DITHIOPHOSPHINIC ACID AND TOPO IN A HOLLOW FIBER MODULE FOR AMERICIUM(II)-LANTHANIDES(III) SEPARATION', Separation Science and Technology, 37: 15, 3369 — 3390
To link to this Article: DOI: 10.1081/SS-120014432
URL: http://dx.doi.org/10.1081/SS-120014432

MARCEL DEKKER, INC. • 270 MADISON AVENUE • NEW YORK, NY 10016

SEPARATION SCIENCE AND TECHNOLOGY
Vol. 37, No. 15, pp. 3369–3390, 2002

MINOR ACTINIDE PARTITIONING BY LIQUID–LIQUID EXTRACTION: USING A SYNERGISTIC MIXTURE OF BIS(CHLOROPHENYL)-DITHIOPHOSPHINIC ACID AND TOPO IN A HOLLOW FIBER MODULE FOR AMERICIUM(II)–LANTHANIDES(III) SEPARATION

Andreas Geist,* Michael Weigl, and Klaus Gompper

Forschungszentrum Karlsruhe GmbH, Institut für Nukleare Entsorgung, P.O. Box 3640, 76021 Karlsruhe, Germany

ABSTRACT

Regarding the difficult selective extraction of trivalent actinides over fission lanthanides from acidic media, we performed several separation tests in hollow fiber modules. Using a synergistic mixture of bis(chlorophenyl)dithiophosphinic acid and tri-*n*-octyl phosphine oxide in *tert*-butyl benzene, tests on extraction, lanthanide scrubbing, and stripping were performed. Up to 99.99% americium could be extracted from 0.5 kmol/m^3 nitric acid, with approximately one third of the lanthanides being co-

*Corresponding author. Fax: +49-7247-82-3927; E-mail: geist@ine.fzk.de

DOI: 10.1081/SS-120014432
0149-6395 (Print); 1520-5754 (Online)

www.dekker.com

MARCEL DEKKER, INC. • 270 MADISON AVENUE • NEW YORK, NY 10016

extracted. Mass transfer calculations using a consistent set of input data showed good agreement with the experiments. The influence of operating mode on extraction efficiency was very pronounced. This is discussed based on the calculations.

Key Words: Actinide(III)-lanthanide separation; Dithiophosphinic acid; Liquid-liquid extraction; Hollow-fiber module; Mass transfer calculations

INTRODUCTION

The radiotoxicity of spent nuclear fuel is governed by its content of plutonium and the minor actinides (neptunium, americium, curium) for several 10^5 years. The partitioning and transmutation strategy[1] aims at minimizing the long-term radiotoxicity by separating these elements (partitioning) and fissioning them to short-lived and eventually stable nuclides (transmutation). Generally, it is foreseen to separate from dissolved spent fuel uranium, plutonium, and neptunium by a slightly modified PUREX (plutonium and uranium recovery by extraction) process. Subsequently, americium and curium are to be separated from the PUREX raffinate. Unfortunately, processes developed for this task so far (e.g., DIAMEX (diamide extaction), TRUEX (transuranium extraction), DIDPA (di-isodecyl phosphoric acid process), TRPO (trialkyl phosphine oxide process)) co-extract trivalent fission lanthanides due to their chemical similarity to the trivalent actinides. The former interfere with the subsequent actinide transmutation, due to their relative abundance (the fission lanthanides/trivalent actinides mass ratio is approximately 20, depending on fuel burn-up) and their large neutron cross sections. Hence, in this context, the separation of trivalent actinides from the fission lanthanides is a key step.

Over the years, efforts have been made to find extractants separating trivalent actinides from fission lanthanides. Few extractants selectively extract trivalent actinides over fission lanthanides with usable distribution coefficient from 0.1 to 1 *M* nitric acid.[2] This range of acidity has to be processed due to nitric acid co-extraction in most of the preceding processes. A synergistic mixture of bis(chlorophenyl)dithiophosphinic acid and tri-*n*-octyl phosphine oxide (TOPO) meets these prerequisites:[3] A mixture of 0.5 kmol/m^3 bis(chlorophenyl)dithiophosphinic acid and 0.25 kmol/m^3 TOPO, dissolved in *tert*-butyl benzene, extracts americium(III) from 0.5 kmol/m^3 nitric acid with a distribution ratio of ≈ 20 and an americium(III)–europium(III) separation factor of ≈ 30.[2] The loaded solvent can be stripped into 1.5–2.0 kmol/m^3 nitric acid.

Bis(chlorophenyl)dithiophosphinic acid, when used without synergist, does not extract or separate americium(III) effectively in this acidity range. The role of the synergist is extensively discussed in Ref. [4] and, regarding bis(2,4,4-trimethylpentyl)dithiophosphinic acid (i.e., purified Cyanex 301), in Ref. [5].

Several counter-current extraction tests in centrifugal extractor batteries were performed by another laboratory using this synergistic mixture. The behavior was promising.[2,6] Alternatively, we implemented hollow fiber modules (HFM) as phase contacting devices for liquid–liquid extraction.[7] Basically, in a HFM, aqueous and organic phases are macroscopically separated by a micro-porous membrane. Phase contact is maintained within the pores by the application of an appropriate pressure difference. This makes for a wide flexibility towards hydrodynamic conditions, overcoming restrictions encountered with conventional extractors, e.g., entrainment.[8]

We performed several extraction tests on americium(III)/lanthanide(III) separation using HFM. Two experiments on extraction, one experiment on lanthanide scrubbing and two stripping experiments were performed in a single-HFM setup[7] installed in a glove box.

Since flow rates have a strong influence on extraction efficiency, they were varied. To investigate the influence of operating mode on separation efficiency, two extraction experiments were performed: aqueous phase flowed either inside the hollow fibers or in the shell-side of the HFM.

The experiments were accompanied by computer code calculations predicting stationary outlet concentrations.[7,9] These calculations take into account fundamental processes. Data input includes feed concentrations, flow rates, equilibrium and kinetic data, viscosities and module geometry.

EXPERIMENTAL

Bis(Chlorophenyl)Dithiophosphinic Acid

The bis(chlorophenyl)dithiophosphinic acid used was prepared by an external laboratory, according to Ref. [10]. Additionally to NMR, the compound's quality was checked by measuring americium and europium distribution coefficients, which agreed with values from Ref. [2].

HFM Experiments

A single-HFM setup (see Fig. 1) was installed in a glove box. Modules were Celgard LiquiCel Extra-Flow type modules (Celgard Inc., Charlotte, NC, USA), operated in a counter-current/cross-flow mode. A module consists of

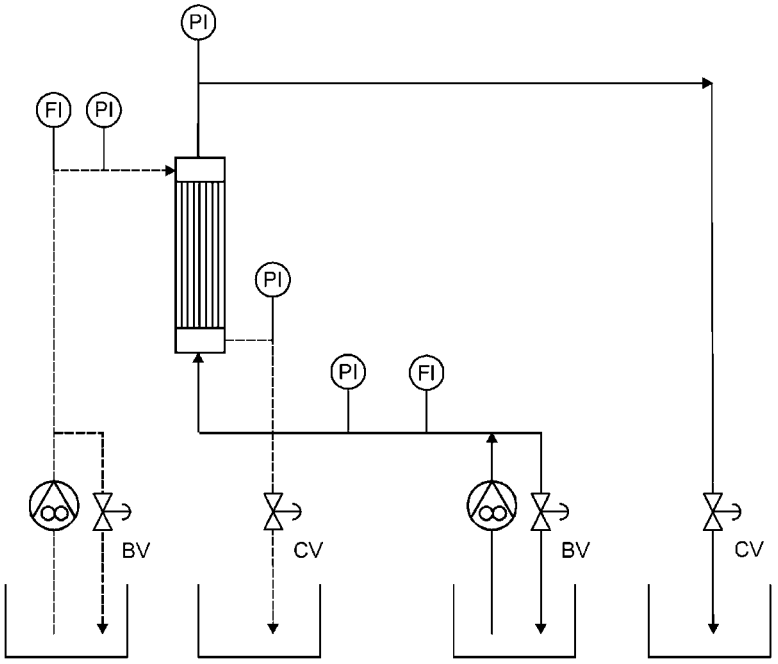

Figure 1. Single-pass, counter-current HFM setup (schematic). — = organic phase, – – = aqueous phase, PI = pressure gauge, FI = flow meter (rotameter), CV = control valve, BP = bypass valve.

10,000 polypropylene hollow fibers having an inner diameter of 0.24 mm and an outer diameter of 0.30 mm. Average pore size is 0.02 μm, porosity is $\varepsilon = 40\%$, tortuosity is $\tau = 2.6$.[11] Active length is 0.15 m. Static pressure in the aqueous phase was kept approximately 0.5 bar higher than in the organic phase to maintain proper phase separation. Both phases passed through the module in single-pass mode, i.e., phases were not recycled.

The experiments were started up by closing the aqueous control valve and filling the module's tube side or shell side (depending on the experiment performed) from the top inlet with aqueous phase, displacing air through the membrane pores. When aqueous feed flow rate dropped to zero, showing that air was displaced completely, the desired flow rate and static pressure was set up. Then the organic phase was introduced from the bottom inlet, displacing air through the organic control valve that was fully opened. When the module was filled completely, organic flow rate was set up. Samples from the aqueous and organic effluents were taken until approximately one liter of each phase was put through. Flow rates were changed and the sampling procedure repeated.

Inlet and outlet americium-241 activities in both phases were measured on a γ-counter (Packard Cobra Auto-Gamma). Lanthanide concentrations were measured with ICP-AES after appropriate dilution in nitric acid (aqueous samples) or stripping into nitric acid (organic samples). Stationary outlet concentrations were plotted vs. flow rate.

HFM Feed Solutions

Aqueous feed for the extraction experiments was a solution of lanthanide nitrates in 0.5 kmol/m^3 nitric acid traced with americium-241. The composition is given in Table 1. Organic phase was a solution of 0.5 kmol/m^3 (160 g/L) bis(chlorophenyl)dithiophosphinic acid and 0.25 kmol/m^3 (97 g/L) TOPO (Aldrich) in *tert*-butyl benzene (Sigma-Aldrich, Deisenhofen, Germany). Scrub solution was 1.0 kmol/m^3 nitric acid, strip solution was either 1.5 or 2.0 kmol/m^3 nitric acid. The loaded organic phase from the first extraction experiment was used in the stripping experiment into 1.5 kmol/m^3 nitric acid. Organic feed for the scrubbing experiment was the loaded organic phase collected from the second extraction experiment. The organic effluent from the scrubbing experiment was

Table 1. Aqueous Feed Loading for Extraction Experiments and Organic Feed Loading for Scrubbing and Stripping Experiments

Compound	Extraction 1 + 2	Scrubbing	Stripping 1	Stripping 2
^{241}Am	876 kBq/L	915 kBq/L	616 kBq/L	591 kBq/L
	6.9 μg/L	7.2 μg/L	4.85 μg/L	4.65 μg/L
	2.86×10^{-5} mol/m^3	2.99×10^{-5} mol/m^3	2.01×10^{-5} mol/m^3	1.93×10^{-5} mol/m^3
Y	221 mg/L	17.5 mg/L	37 mg/L	9.7 mg/L
	2.49 mol/m^3	0.197 mol/m^3	0.42 mol/m^3	0.11 mol/m^3
La	756 mg/L	82 mg/L	72 mg/L	36 mg/L
	5.44 mol/m^3	0.59 mol/m^3	0.52 mol/m^3	0.26 mol/m^3
Ce	1460 mg/L	306 mg/L	247 mg/L	139 mg/L
	10.4 mol/m^3	2.18 mol/m^3	1.76 mol/m^3	0.992 mol/m^3
Pr	699 mg/L	143 mg/L	118 mg/L	66.5 mg/L
	4.96 mol/m^3	1.01 mol/m^3	0.837 mol/m^3	0.472 mol/m^3
Nd	2512 mg/L	312 mg/L	284 mg/L	145 mg/L
	17.4 mol/m^3	2.16 mol/m^3	1.97 mol/m^3	1.01 mol/m^3
Sm	457 mg/L	74 mg/L	64 mg/L	35 mg/L
	3.04 mol/m^3	0.49 mol/m^3	0.43 mol/m^3	0.23 mol/m^3
Eu	91 mg/L	14 mg/L	15 mg/L	6.8 mg/L
	0.60 mol/m^3	0.092 mol/m^3	0.099 mol/m^3	0.045 mol/m^3
Gd	55 mg/L	15 mg/L	8.5 mg/L	6.9 mg/L
	0.35 mol/m^3	0.095 mol/m^3	0.054 mol/m^3	0.044 mol/m^3

used as feed in the stripping experiment into 2.0 kmol/m^3 nitric acid. Loading of the organic phases is given in Table 1.

The viscosity of the organic phase was determined to be $\nu = 2.6 \times 10^{-6}$ m^2/sec (20°C) using an Ubbelohde viscosimeter. The density was $\rho = 924$ kg/m^3 (20°C).

MASS TRANSFER SYSTEM AND HFM MASS TRANSFER CALCULATIONS

Outline

Calculations were performed to determine steady-state effluent concentrations. These are based on equilibrium and kinetic data, diffusion coefficients, and a hydrodynamic description of the module. The calculations are described in detail in Ref. [7] for single-cation extraction. They were extended for multi-cation co-extraction, analogous to Ref. [9].

The module was divided into an appropriate number of cells. In each of these, individual mass transfer coefficients for all species involved were calculated from hydrodynamic and diffusion data. With equilibrium data, individual mass transfer coefficients and module geometry, changes in concentration in each cell due to mass transfer across the liquid–liquid interface were calculated. Tube and shell side cell concentrations were then passed on stepwise, and again, fluxes were calculated, until steady state was attained.

Mass Transfer System

The mass transfer system, which is rather complicated[3] was simplified to a liquid ion-exchange system with the following stoichiometry:

$$Me^{3+}_{aq} + 2(HX)_{2,org} \rightleftharpoons MeX_3 \cdot HX_{org} + 3H^+_{aq} \quad (1)$$

This stoichiometry was also reported for the extraction of americium and europium with bis(2,4,4-trimethylpentyl)dithiophosphinic acid,[12] and was further confirmed by an EXAFS investigation.[13] However, a recent investigation[14] concludes that also the following stoichiometry is reasonable:

$$Me^{3+}_{aq} + 3HX_{org} \rightleftharpoons MeX_{3org} + 3H^+_{aq} \quad (2)$$

However, due to the relatively low loading of the organic phase (approximately 10% due to lanthanide co-extraction, see "Results from Experiments and Calculations"), this has no significant impact on the calculations.

Finally, it was checked experimentally that nitric acid co-extraction, which might have been expected due to TOPO,[15] did not occur.

Kinetics of Mass Transfer

Kinetic investigations performed in a stirred cell indicated that the rate of both americium and europium mass transfer is controlled by diffusion in the range of hydrodynamic conditions considered here for both extraction and back extraction.[16,17] Hence, chemical equilibrium is established at the interface. Only diffusive mass transfer and not the rate of the chemical reaction needed to be implemented in the calculations.

Flux Equations

For $Me_i^{3+} = Am^{3+}$ or Ln^{3+}, the following mass transfer resistances were taken into account:

1. Transport of metal ions and protons, either inside HF or shell-side

$$j_{Me_i^{3+}} = k_{Me_i^{3+}}([Me_i^{3+}] - [Me_i^{3+}]^*) \quad (3)$$

$$j_{H^+} = k_{H^+}([H^+]^* - [H^+]) \quad (4)$$

2. Diffusion of metal complexes and complexant in the pores of the hydrophobic membrane material

$$j_{Me_iX_3\cdot HX,M} = \frac{D_{Me_iX_3\cdot HX}\cdot\varepsilon}{d\cdot\tau}([Me_iX_3\cdot HX]^* - [Me_iX_3\cdot HX]^{**}) \quad (5)$$

$$j_{(HX)_2,M} = \frac{D_{(HX)_2}\cdot\varepsilon}{d\cdot\tau}([(HX)_2]^{**} - [(HX)_2]^*) \quad (6)$$

3. Transport of metal complexes and complexant, either shell-side or in the lumen of HF

$$j_{Me_iX_3\cdot HX} = k_{Me_iX_3\cdot HX}([Me_iX_3\cdot HX]^{**} - [Me_iX_3\cdot HX]) \quad (7)$$

$$j_{(HX)_2} = k_{(HX)_2}\cdot([(HX)_2] - [(HX)_2]^{**}) \quad (8)$$

Individual fluxes j_i were coupled according to the stoichiometry of the ion-exchange reaction at the interface [Eq. (1)] and the membrane geometry. With this, individual interfacial equilibrium conditions K_i for all Me_i^{3+} involved were

rewritten using interfacial concentrations,

$$[Me_i^{3+}]^* = [Me_i^{3+}] - \frac{j_{Me_i^{3+}}}{k_{Me_i^{3+}}} \tag{9}$$

$$[H^+]^* = [H^+] + \frac{3 \cdot \sum j_{Me_i^{3+}}}{k_{H^+}} \tag{10}$$

$$[Me_iX_3 \cdot HX]^* = [Me_iX_3 \cdot HX] + j_{Me_i^{3+}} \cdot \left(\frac{A^*}{k_{Me_iX_3 \cdot HX} \cdot A^{**}} + \frac{d \cdot \tau \cdot A^*}{D_{Me_iX_3 \cdot HX} \cdot \varepsilon \cdot A_M} \right) \tag{11}$$

$$[(HX)_2]^* = [(HX)_2] - \sum (2 \cdot j_{Me_i^{3+}}) \left(\frac{A^*}{k_{(HX)_2} \cdot A^{**}} + \frac{d \cdot \tau \cdot A^*}{D_{(HX)_2} \cdot \varepsilon \cdot A_M} \right) \tag{12}$$

corresponding to

$$K_i = \frac{\left\{ [Me_iX_3 \cdot HX] + j_{Me_i^{3+}} \left(\frac{A^*}{k_{Me_iX_3 \cdot HX} \cdot A^{**}} + \frac{d \cdot \tau \cdot A^*}{D_{Me_iX_3 \cdot HX} \cdot \varepsilon \cdot A_M} \right) \right\} \left\{ [H^+] + \frac{3 \cdot \sum j_{Me_i^{3+}}}{k_{H^+}} \right\}^3}{\left\{ [Me_i^{3+}] - \frac{j_{Me_i^{3+}}}{k_{Me_i^{3+}}} \right\} \left\{ [(HX)_2] - \sum (2 \cdot j_{Me_i^{3+}}) \cdot \left(\frac{A^*}{k_{(HX)_2} \cdot A^{**}} + \frac{d \cdot \tau \cdot A^*}{D_{(HX)_2} \cdot \varepsilon \cdot A_M} \right) \right\}^2} \tag{13}$$

with $A_M = (A^* + A^{**})/2$.

All K_i are coupled by the common proton and complexant interfacial concentrations, $[H^+]^*$ and $[(HX)_2]^*$. The sum terms in Eq. (13) express the mutual influence of co-extracted cations on mass transfer in the multi-cation extraction system.

Hence, with equilibrium data, diffusion coefficients, and individual mass transfer coefficients known, fluxes j of the key components could be calculated numerically.

Equilibrium Data

Equilibrium data were taken from Ref. [2]. They are compiled in Fig. 2. Using these and the above stoichiometry [cf. Eq. (1)], the americium equilibrium constant was derived, $K_{Am} = 23.8$. Since the fission lanthanides are extracted rather unselectively, an average equilibrium constant, K_{Ln} was used. However,

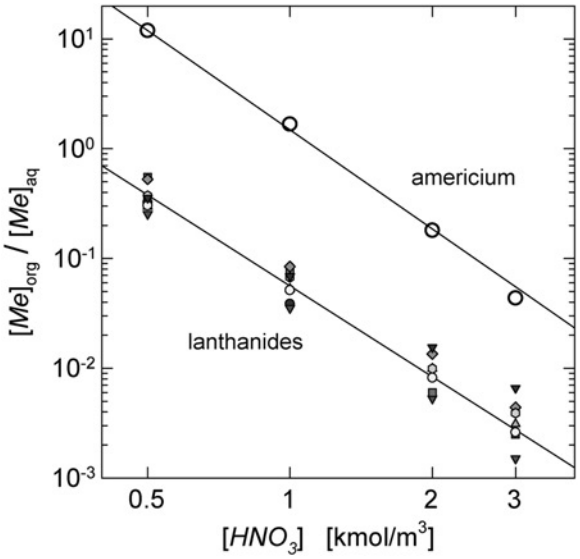

Figure 2. Equilibrium distribution ratios as a function of nitric acid concentration, taken from Ref. [2]. Aqueous phase: Am-241 tracer + fission lanthanides according to Table 1, column "Extraction 1 + 2." Organic phase: 0.5 kmol/m^3 bis(chlorophenyl)dithiophosphinic acid + 0.25 kmol/m^3 TOPO in *tert*-butyl benzene. Symbols: experiment (legend see Fig. 4), lines: calculated with equilibrium data.

the slope of the acid dependency for the lanthanides was not 3 as expected. Data from Ref. [2] could best be fit using a slope of 2.75, which was confirmed by own measurements. $K_{Ln} = 0.9$ best described the data. Regarding lanthanides extraction, a proton dependency of 2.75 instead of 3 was used in Eqs. (1) and (13).

Diffusion Coefficients

Aqueous diffusion coefficients used were: $D_{Am} = D_{Ln} = 6.2 \times 10^{-10}$ m^2/sec,[18,19] $D_H = 9{\cdot}10^{-9}$ m^2/sec.[20] A complexing agent dimer diffusion coefficient of $D_{HX} = 2{\cdot}10^{-10}$ m^2/sec was estimated using the Wilke–Chang correlation.[21] Assuming the metal complexes have approximately a molecular volume three times that of the complexant dimer, metal complex diffusion coefficients were estimated to $D_{AmX} = D_{LnX} = 1 \times 10^{-10}$ m^2/sec. However, to better describe the experimental data, $D_{HX} = 2.5 \times 10^{-10}$ m^2/sec and $D_{AmX} = D_{LnX} = 1.25 \times 10^{-10}$ m^2/sec were used in the calculations.

Individual Mass Transfer Coefficients

Mass transfer coefficients in the lumen of HF were calculated according to an analytical solution reported in Ref. [22]. Since cross-flow modules were used in this work, the calculations were adapted to the radial flow in the shell-side of these modules. A shell-side mass transfer correlation that takes into account the hydrodynamics of these modules was used.[23]

RESULTS FROM EXPERIMENTS AND CALCULATIONS

Considering that all calculations were performed using one set of input data, the agreement of the calculated and the experimental extraction efficiencies was good throughout the five experiments performed. With the exception of the scrubbing test, the calculations tended to be slightly conservative.

Mass balances are stated as a control for the quality of the experiment. At steady state conditions, the sum of mass fluxes in both effluents should be equal to the feed mass flux, and MB = 100%, with

$$\mathrm{MB} = \frac{([\mathrm{Me}]_{\mathrm{aq,\,out}} \cdot Q_{\mathrm{aq}} + [\mathrm{Me}]_{\mathrm{org,\,out}} \cdot Q_{\mathrm{org}})}{([\mathrm{Me}]_{\mathrm{in}} \cdot Q_{\mathrm{feed}})} \cdot 100\%$$

with $Q_{\mathrm{feed}} = Q_{\mathrm{aq}}$ and $[\mathrm{Me}]_{\mathrm{in}} = [\mathrm{Me}]_{\mathrm{aq,\,in}}$ for extraction, and $Q_{\mathrm{feed}} = Q_{\mathrm{org}}$ and $[\mathrm{Me}]_{\mathrm{in}} = [\mathrm{Me}]_{\mathrm{org,\,in}}$ for scrubbing and stripping.

Extraction Experiment 1

In the first extraction test, the aqueous phase was flowing in the shell side of the HFM. Equal aqueous and organic flow rates, $Q_{\mathrm{aq}} = Q_{\mathrm{org}}$, were varied: 400, 800, and 1500 mL/hr.

Mass balances were 91–95% (americium) and 96–103% (lanthanides). Aqueous effluent concentrations normalized to aqueous feed concentrations, $[\mathrm{Me}]_{\mathrm{aq,\,out}}/[\mathrm{Me}]_{\mathrm{aq,\,in}}$, as a function of flow rate, Q, are shown in Fig. 3. With a flow rate of 400 mL/hr, 97.5% of americium could be extracted, with approximately 30% of the lanthanide inventory being co-extracted. Increasing flow rate decreased extraction efficiency, due to the reduced residence time of the phases in the HFM.

Extraction Experiment 2

In the second extraction test, the aqueous phase was flowing inside the hollow fibers, other than in the first extraction test. Aqueous flow rate was varied,

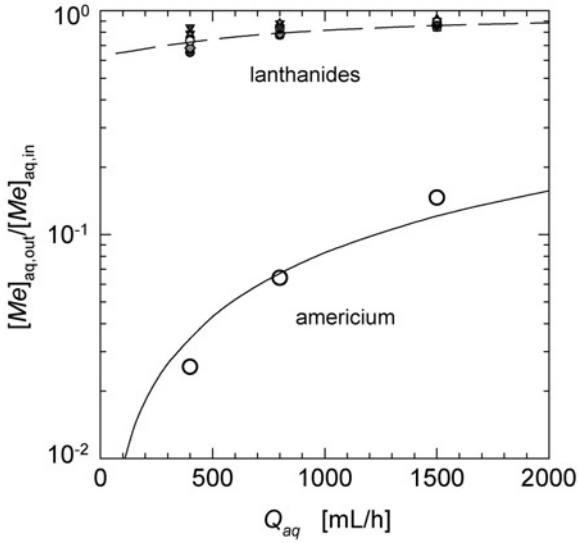

Figure 3. HFM extraction Experiment 1. Aqueous phase shell-side, $Q_{org} = Q_{aq}$. Aqueous phase: 0.5 kmol/m^3 nitric acid, loaded according to Table 1. Organic phase: 0.5 kmol/m^3 bis(chlorophenyl)dithiophosphinic acid + 0.25 kmol/m^3 TOPO in *tert*-butyl benzene. Symbols: experiment (legend see Fig. 4), — = americium calculated, – – = lanthanides calculated.

$Q_{aq} = 300$, 490, and 800 mL/hr. Organic flow rate was kept constant at $Q_{org} = 300$ mL/hr.

Mass balances were 100–103% (americium) and (100 ± 5%) (lanthanides). The change in operating mode drastically improved the extraction efficiency: 99.99% of americium could be removed at $Q_{aq} = 300$ mL/hr (see Fig. 4). Again, approximately 30% of the lanthanides was co-extracted. Flow rate dependency of extraction efficiency was more pronounced than in the first extraction experiment. The reason for this behavior is given below.

Influence of Operating Mode

Figure 5 compares calculations regarding extraction Experiments 1 and 2, demonstrating the influence of operating mode on extraction efficiency. Contrary to the experiments, $Q_{aq} = Q_{org}$ in both cases to isolate the effect of operating mode. Although lanthanide extraction is practically not affected, the effect for americium is tremendous. It is evident that, especially at lower flow rates, it is

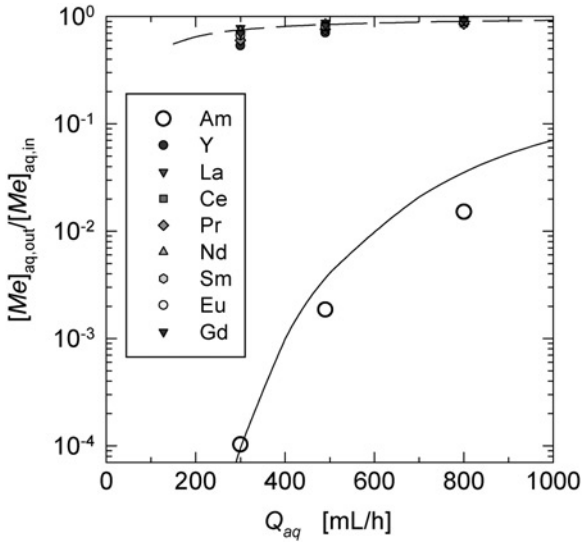

Figure 4. HFM extraction Experiment 2. Aqueous phase inside HF, $Q_{org} = 300\,mL/hr$. Aqueous phase: $0.5\,kmol/m^3$ nitric acid, loaded according to Table 1. Organic phase: $0.5\,kmol/m^3$ bis(chlorophenyl)dithiophosphinic acid + $0.25\,kmol/m^3$ TOPO in *tert*-butyl benzene. Symbols: experiment, — = americium calculated, – – = lanthanides calculated.

advantageous to lead the aqueous phase inside the hollow fibers. This can be explained by the influence of flow rate on mass transfer coefficients, which is different depending on operating mode.

For the applied conditions, overall americium mass transfer resistance is given mainly by diffusion of metal ions in the aqueous phase. Investigating the sensitivity of diffusion coefficients on calculated extraction efficiency proved this: only the metal-ion diffusion coefficient had a significant influence. Hence, the further considerations can be confined to the aqueous phase.

This means that, for given module geometry and chemical conditions, extraction efficiency is basically influenced by the mass transfer coefficient of metal ions, k_{Me}, and the residence time of the aqueous phase.

Local mass transfer coefficients in the lumen of hollow fibers are calculated according to an analytical solution.[22] They are dependent on flow velocity only in the entrance region, converging towards a constant value (here: $k_{Me} = 9.2 \times 10^{-6}\,m/sec$ for a hollow fiber inner diameter of 240 μm and a diffusivity of $6.2 \times 10^{-10}\,m^2/sec$) as the concentration profile fully develops. The length of the

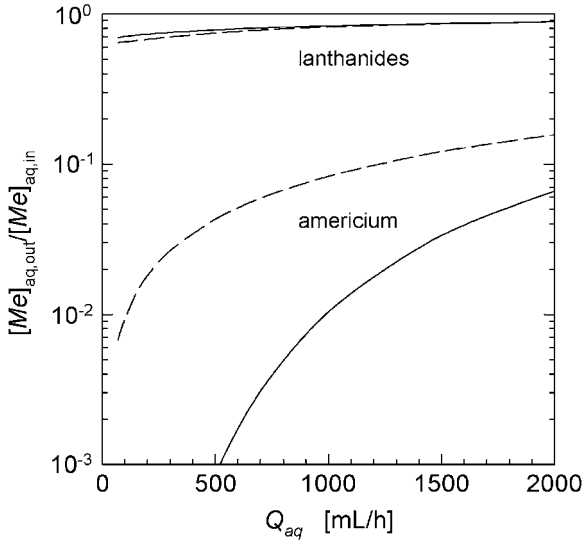

Figure 5. HFM calculations on the influence of operating mode on extraction efficiency. $Q_{aq} = Q_{org}$. — = Aqueous phase inside HF, – – = aqueous phase shell-side.

entrance region in which the concentration profile develops is

$$L_c = 0.05 \cdot Re \cdot Sc \cdot d_i.$$[24]

Hence, $L_c = 2.86 \times 10^{-3}$ m at a flow rate of 1000 mL/hr, i.e., the concentration profile fully develops within 2% of the fiber length. This means that the mean mass transfer coefficient inside the hollow fibers is practically not flow rate dependent on the range of relevant flow rates, and extraction efficiency is governed by the aqueous phase residence time.

Local shell-side mass transfer coefficient is calculated according to an empirical correlation,[23]

$$Sh = k_{Me} \cdot d_i / D_{Me} = 1.76 \cdot Re^{0.82} \cdot Sc^{0.33}$$

It is strongly dependent on throughput (cf. the exponent of the Reynolds number in the proceeding equation), compensating the influence of residence time to some extent. That is, as aqueous flow rate increases, residence time decreases, whereas the mass transfer coefficient increases. This is the reason for the less steep extraction efficiency dependency on flow rate if the aqueous phase flows shell-side.

Now comparing tube-side and shell-side aqueous metal-ion mass transfer coefficients, the tube-side coefficient is $k_{Me} = 9.2 \times 10^{-6}$ m/sec, independent of flow rate. The shell-side coefficient is in the range of $k_{Me} \approx 2 \times 10^{-6}$ m/sec at $Q_{aq} = 1000$ mL/hr, $k_{Me} \approx 1 \times 10^{-6}$ m/sec at $Q_{aq} = 500$ mL/hr, and $k_{Me} \approx 7 \times 10^{-7}$ m/sec at $Q_{aq} = 300$ mL/hr, respectively. Hence, it is obvious that extraction is more efficient if the aqueous phase flows in the lumen of the hollow fibers.

Analogously, these considerations are also valid for scrubbing and back-extraction, leading to the overall conclusion that it is advantageous to flow the feed phase inside the hollow fibers, at least at low flow rates where extraction efficiency is highest.

Scrubbing Experiment

An experiment on lanthanide scrubbing was performed, contacting the loaded organic phase from the second extraction test with 1.0 kmol/m^3 nitric acid. By mistake, the organic phase flowed shell-side (it was intended to flow the organic phase in the lumen of HF). Aqueous and organic flow rates were equal, $Q_{aq} = Q_{org}$. They were varied, as 300, 490, and, 820 mL/hr.

Mass balances were (100 ± 1%) for americium, (100 ± 5%) for yttrium, and 89–94% for the lanthanides. Approximately 70% of the lanthanides could be scrubbed from the organic phase at 300 mL/hr. Forty-five percent of americium was also scrubbed from the organic phase, see Fig. 6.

The calculations suggest that flowing the organic phase inside the hollow fibers would have resulted in a much better lanthanide scrubbing efficiency, without influencing americium scrubbing (cf. the dash-dotted lines in Fig. 6).

Stripping Experiment 1

Two HFM stripping tests were performed. In the first stripping experiment, the loaded organic phase from the first extraction experiment was contacted with 1.5 kmol/m^3 nitric acid. The organic phase flowed in the lumen of the hollow fibers. Aqueous and organic flow rates were equal, $Q_{aq} = Q_{org}$. They were varied, 300, 800, and, 1500 mL/hr.

Mass balances were 100–108% for americium and 100–114% for the lanthanides. Eighty percent of americium and approximately 93% of the lanthanides (except yttrium, 88%) could be stripped from the organic phase at 300 mL/hr, see Fig. 7.

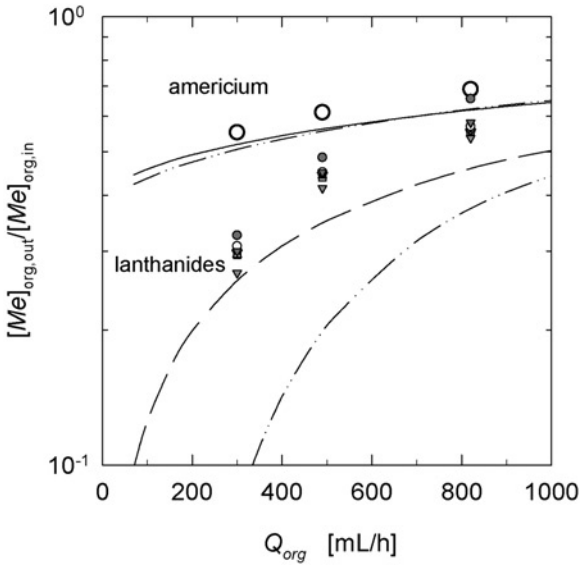

Figure 6. HFM scrubbing experiment. Organic phase shell-side, $Q_{aq} = Q_{org}$. Scrubbing phase: 1.0 kmol/m^3 nitric acid. Organic phase: 0.5 kmol/m^3 bis(chlorophenyl)dithiophosphinic acid + 0.25 kmol/m^3 TOPO in *tert*-butyl benzene, loaded according to Table 1. Symbols: experiment (legend see Fig. 4), — = americium calculated, – – = lanthanides calculated, —··—··— = calculated (organic phase inside HF).

Stripping Experiment 2

In the second stripping test, the organic effluent from the scrubbing experiment was stripped into 2.0 kmol/m^3 nitric acid. Again, the organic phase flowed in the lumen of the hollow fibers. Equal aqueous and organic flow rates, $Q_{aq} = Q_{org}$, were varied: 320, 490, and, 810 mL/hr.

Mass balances were 97–99% for americium and (100 ± 5%) for the lanthanides. At 320 mL/hr, 88% of americium and 93–95% of the lanthanide inventory could be stripped from the organic phase, see Fig. 8. Regarding americium stripping, this is a slight improvement over the first stripping test, due to the increase in nitric acid concentration. Lanthanide stripping performance is not further improved since lanthanides distribute almost completely to the aqueous phase even at 1.5 kmol/m^3 nitric acid, cf. Fig. 2.

To achieve more complete stripping, significantly lower flow rates would be required. The calculations indicate that to achieve, e.g., 99% stripping efficiency, stripping has to be performed at a flow rate of 100 mL/hr.

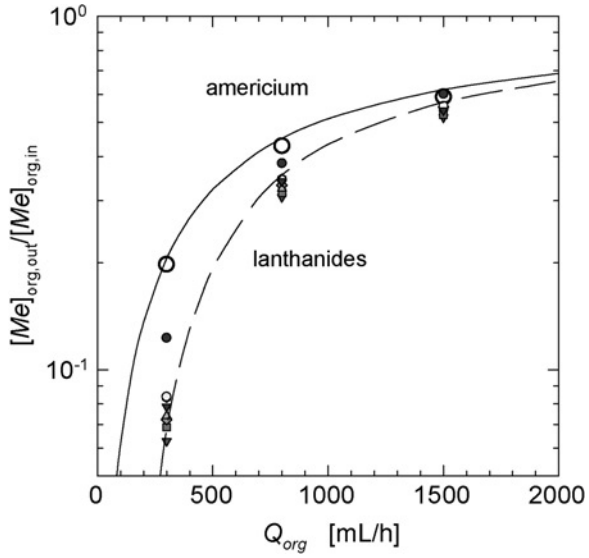

Figure 7. HFM stripping Experiment 1. Organic phase inside HF, $Q_{aq} = Q_{org}$. Stripping phase: 1.5 kmol/m^3 nitric acid. Organic phase: 0.5 kmol/m^3 bis(chlorophenyl)dithiophosphinic acid + 0.25 kmol/m^3 TOPO in *tert*-butyl benzene, loaded according to Table 1. Symbols: experiment (legend see Fig. 4), — = americium calculated, – – = lanthanides calculated.

Extraction Efficiency vs. Stripping Efficiency

As shown in Fig. 4, 99.99% of americium can be removed from 0.5 kmol/m^3 nitric acid at a flow rate of 300 mL/hr. The respective americium distribution coefficient is approximately 20 (cf. Fig. 2). On the other hand, only approximately 95% of the lanthanides can be stripped into 2.0 kmol/m^3 nitric acid at comparable flow rate (cf. Fig. 8), despite the fact that the respective distribution coefficients for the lanthanides are in the range of 0.01.

The lower efficiency regarding stripping is attributable to the following facts: Extraction overall mass transfer resistance is controlled mainly by the diffusion of the metal ions in the aqueous phase. On the other hand, stripping overall mass transfer resistance is controlled by the diffusion of the metal complexes in the organic phase. This could be proved by sensitivity calculations varying aqueous and organic diffusivities. Hence, stripping is governed by the slow diffusion of metal complexes (organic complex diffusivities are approximately five times lower than metal-ion diffusivities, cf. "HFM Mass

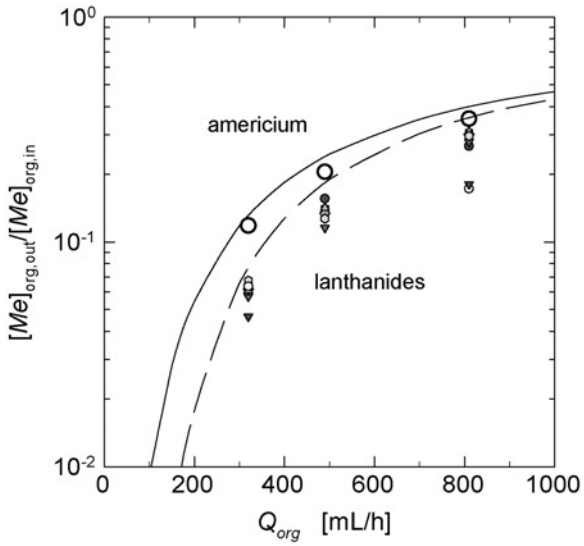

Figure 8. HFM stripping Experiment 2. Organic phase inside HF, $Q_{aq} = Q_{org}$. Stripping phase: 2.0 kmol/m^3 nitric acid. Organic phase: 0.5 kmol/m^3 bis(chlorophenyl)dithiophosphinic acid + 0.25 kmol/m^3 TOPO in *tert*-butyl benzene, loaded according to Table 1. Symbols: experiment (legend see Fig. 4), — = americium calculated, – – = lanthanides calculated.

Transfer Calculations"). It is additionally impeded by the diffusive resistance in the membrane pores, which are wetted with organic phase.

Proposed Flowsheet

To make partitioning and transmutation a success, trivalent actinides must be separated to >99.9%. However, lanthanide co-extraction must be suppressed, due to their relative abundance and their large neutron cross sections. As a first approach, targeted decontamination factors are $DF_{Am} > 1000$, and $DF_{Ln} > 400$, for an actinide(III)–lanthanide(III) separation process. Decontamination factors are defined as

$$DF_{Am} = \frac{([Am]_{feed} \cdot Q_{feed})}{([Am]_{raffinate} \cdot Q_{raffinate})} \quad \text{with} \quad Q_{raffinate} = Q_{feed} + Q_{scrub}$$

$$DF_{Ln} = \frac{([Ln]_{feed} \cdot Q_{feed})}{([Ln]_{product} \cdot Q_{product})} \quad \text{with} \quad Q_{product} = Q_{strip}$$

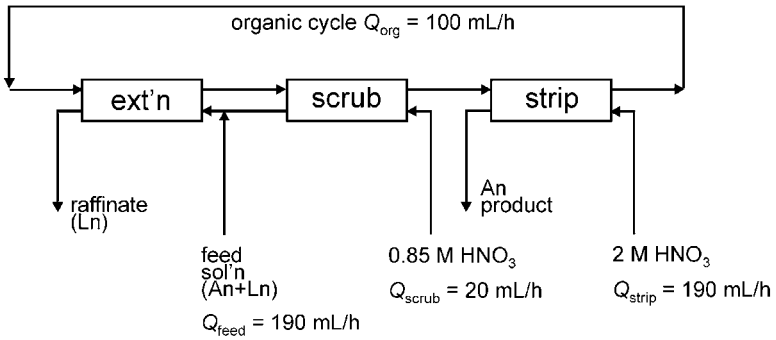

Figure 9. Proposed flowsheet consisting of three coupled HFM for extraction, scrubbing, and stripping. Feed composition according to Table 1, column "Extraction 1 + 2," in 0.5 kmol/m^3 nitric acid. Organic phase: 0.5 kmol/m^3 bis(chlorophenyl)dithiophosphinic acid + 0.25 kmol/m^3 TOPO in *tert*-butyl benzene.

Using the above calculations, a flowsheet was developed for continuous americium(III)–lanthanides separation. Three HFM were coupled as shown in Fig. 9. Aqueous feed was 0.5 kmol/m^3 nitric acid, loaded according to Table 1, column "Extraction 1 + 2" (i.e., a total lanthanide concentration of 6250 mg/L), with a flow rate of $Q_{\text{feed}} = 190\,\text{mL/hr}$. Scrubbing and stripping solutions were 0.85 and 2.0 kmol/m^3 nitric acid, at $Q_{\text{scrub}} = 20\,\text{mL/hr}$ and $Q_{\text{strip}} = 190\,\text{mL/hr}$, respectively. Organic phase was 0.5 kmol/m^3 bis(chlorophenyl)dithiophosphinic acid +0.25 kmol/m^3 TOPO in *tert*-butyl benzene, at $Q_{\text{org}} = 100\,\text{mL/hr}$. Organic phase was recycled. In the extraction module, aqueous phase flowed inside the hollow fibers. In the scrubbing and stripping modules, aqueous phase flowed shell-side.

The calculated performance of this flowsheet is $\text{DF}_{\text{Am}} = 1130$, and $\text{DF}_{\text{Ln}} = 410$, thus meeting the demanded decontamination factors. The relative americium and lanthanide mass flow fractions in the effluents and in the organic recycle are given in Table 2.

Table 2. Calculated Relative Americium and Lanthanide Mass Fractions in the Effluents and in the Organic Recycle

Compound	Raffinate	Product	Solvent	Sum
Americium	8.84×10^{-4}	0.9992	1.11×10^{-3}	1.001
Lanthanides	0.9974	2.44×10^{-3}	7.75×10^{-7}	0.9998

CONCLUSIONS

Due to its good separation factor and rapid mass transfer, the extraction system used is well suited for americium(III)–lanthanide(III) separation. HFM showed good extraction performance, especially regarding americium removal, which was up to four orders of magnitude. Whether the feed phase flows inside the hollow fibers or in the shell-side, has a pronounced effect on extraction efficiency. This could be explained by the flow rate dependency of mass transfer coefficients being different, depending on operating mode.

Scrubbing and stripping were also successful, although they would have to be performed at lower flow rates compared to extraction. This is due to the lower values of organic diffusion coefficients. However, since flow rates and flow ratios are totally flexible in a HFM, conditions for complete stripping can easily be selected. As expected from HFM operation, no organic phase was entrained in the aqueous effluent. The calculations were in good agreement with the experiments. Except with the scrubbing experiment, the calculations tended to slightly underpredict mass transfer efficiency. The fact that only one set of data was used throughout the calculations is important for scale-up.

With these calculations, a flowsheet was developed, giving an americium decontamination factor of $DF_{Am} = 1130$, and a lanthanide decontamination factor of $DF_{Ln} = 410$. This demonstrates the potential of a continuous HFM extraction process using a synergistic mixture of bis(chlorophenyl)dithiophosphinic acid and TOPO for americium(III)–lanthanide separation.

NOMENCLATURE

A	membrane area (m^2)
D	diffusion coefficient (m^2/sec)
d	membrane wall thickness (m)
d_i	inner HF diameter (m)
DF	decontamination factor (—)
ε	porosity (—)
HF	hollow fiber
HFM	hollow fiber module
HX	extractant monomer
j	flux (kmol/m^2 sec)
k	mass transfer coefficient (m/sec)
L_c	concentration profile developing length (m)
K	equilibrium constant, here: (kmol/m^3)
MB	mass balance (—)
Me^{3+}	metal cation, here: Am^{3+}, Ln^{3+}

ν	kinematic viscosity (m^2/sec)
Q	flow rate (mL/hr)
Re	Reynolds number, here: $Re = w \cdot d_i / \nu$ (—)
ρ	density (kg/m^3)
Sc	Schmidt number, $Sc = \nu / D$ (—)
Sh	Sherwood number, here: $Sh = k \cdot d_i / D$ (—)
SF	separation factor (—)
τ	tortuosity (—)
w	linear velocity (m/sec)
[ ]	concentration ($kmol/m^3$) or (mg/L)
aq	in aqueous phase
in	at inlet (feed)
out	at outlet (effluent)
org	in organic phase
*	at liquid/liquid interface, (aqueous phase inside HF: inner membrane surface), (organic phase inside HF: outer membrane surface)
**	at outer membrane surface if aqueous phase flows inside HF, at inner membrane surface if organic phase flow inside HF

ACKNOWLEDGMENTS

The authors are grateful for the financial support from the Commission of the European Community (contract FIKW-CT2000-00087).

REFERENCES

1. *Actinide and Fission Product Partitioning and Transmutation, Status and Assessment Report*; OECD Nuclear Energy Agency: Paris, 1999.
2. Madic, C.; Hudson, M.J.; Liljenzin, J.O.; Glatz, J.P.; Nannicini, R.; Facchini, A.; Kolarik, Z.; Odoj, R. *New Partitioning Techniques for Minor Actinides, EUR 19149*; European Commission: Luxembourg, 2000.
3. Modolo, G.; Odoj, R. Synergistic Selective Extraction of Actinides(III) over Lanthanides from Nitric Acid Using New Aromatic Diorganyldithiophosphinic Acids and Neutral Organophosphorus Compounds. Solvent Extr. Ion Exch. **1999**, *17* (1), 33–53.
4. Ionova, G.; Ionov, S.; Rabbe, C.; Hill, C.; Madic, C.; Guillaumont, R.; Modolo, G.; Krupa, J.C. Mechanism of Trivalent Actinide/Lanthanide Separation Using Synergistic Mixtures of Di(Chlorophenyl)dithiophosphinic Acid and Neutral O-bearing Co-extractants. New J. Chem. **2001**, *25*, 491–501.

5. Ionova, G.; Ionov, S.; Rabbe, C.; Hill, C.; Madic, C.; Guillaumont, R.; Krupa, J.C. Mechanism of Trivalent Actinide/Lanthanide Separation Using bis(2,4,4-Trimethylpentyl)dithiophosphinic Acid (Cyanex 301) and Neutral O-bearing Co-extractant Synergistic Mixtures. Solvent Extr. Ion Exch. **2001**, *19* (3), 391–414.
6. Modolo, G.; Odoj, R.; Baron, P. The ALINA-Process for An(III)/Ln(III) Group Separation from Strong Acidic Medium, In Proceedings of the International Conference on Future Nuclear Systems (GLOBAL 99), Jackson Hole, Wyoming, USA, Aug 29–Sept 3, 1999.
7. Daiminger, U.; Geist, A.; Nitsch, W.; Plucinski, P. The Efficiency of Hollow Fiber Modules for Nondispersive Chemical Extraction. Ind. Eng. Chem. Res. **1996**, *35*, 184–191.
8. Stevens, G.W.; Pratt, H.R.C. Solvent Extraction Equipment Design and Operation: Future Directions from an Engineering Perspective. Solvent Extr. Ion Exch. **2000**, *18* (6), 1051–1078.
9. Geist, A.; Plucinski, P.; Nitsch, W. Modeling of Multi-cation Co-extraction in Hollow-Fiber Modules Based on Kinetic Measurements and Equilibrium Data. Chem.-Ing.-Tech. **1997**, *69* (7), 946–951.
10. Higgins, W.A.; Vogel, P.W.; Craig, W.G. Aromatic Phosphinic Acids and Derivatives. J. Am. Chem. Soc. **1955**, *77*, 1864–1866.
11. Prasad, R.; Sirkar, K.K. Dispersion-Free Solvent Extraction with Microporous Hollow-Fiber Modules. AIChE J. **1988**, *34* (2), 177–188.
12. Zhu, Y.; Chen, J.; Jiao, R. Extraction of Am(III) and Eu(III) from Nitrate Solution with Purified Cyanex 301. Solvent Extr. Ion Exch. **1996**, *14* (1), 61–68.
13. Tian, G.; Zhu, Y.; Xu, J.; Hu, T.; Xie, Y.J. Characterization of Extraction Complexes of Am(III) with Dialkyldithiophosphinic Acids by Extended X-Ray Absorption Fine Structure Spectroscopy. J. Alloys Compounds **2002**, *334*, 86–91.
14. Cote, G.; Martin, J.-V.; Bauer, D.; Mottot, Y. Physico-Chemical Properties of Cyanex 301. In *Proceedings of the International Solvent Extraction Conference (ISEC 2002), Cape Town, South Africa, March 17–21, 2002*; Sole, K.C., Cole, P.M., Preson, J.S., Robinson, D.J., Eds.; South African Institute of Mining and Metallurgy: Johannesburg, South Africa, 2002; 291–298.
15. Marcus, Y.; Kertes, A.S.; Yanir, E. *Equilibrium Constants of Liquid–Liquid Distribution Reactions, Part 1*; Butterworths: London, 1974.
16. Geist, A.; Weigl, M.; Gompper, K. Actinide(III)/Lanthanide(III) Separation in a Hollow Fiber Module with a Synergistic Mixture of bis(Chlorophenyl)dithiophosphinic Acid and TOPO, In Proceedings of the International Conference on Back End of the Fuel Cycle (GLOBAL 2001), Paris, France, Sept 9–13, 2001.

17. Weigl, M. *Current work*.
18. Lide, D.R. *Handbook of Chemistry and Physics*, 75th Ed.; CRC Press: Boca Raton, 1994.
19. Fourest, B.; Duplessis, J.; David, F. Coefficient de Diffusion Limite et Rayon Hydraté de Eu^{3+}, Am^{3+}, Cm^{3+}, Cf^{3+} et Es^{3+}. J. Less-Common Metals **1983**, *92* (1), 17–27.
20. Mills, R.; Lobo, V.M.M. *Self-Diffusion in Electrolyte Solutions*; Elsevier: Amsterdam, 1989.
21. Wilke, C.R.; Chang, P. Correlation of Diffusion Coefficients in Dilute Solutions. AIChE J. **1955**, *1* (2), 264–270.
22. Skelland, A.H.P. *Diffusional Mass Transfer*; John Wiley & Sons: New York, 1974; 159–167.
23. Schöner, P.; Plucinski, P.; Nitsch, W.; Daiminger, U. Mass Transfer in the Shell Side of Cross Flow Hollow Fiber Modules. Chem. Eng. Sci. **1998**, *53* (13), 2319–2326.
24. Rohsenow, W.M.; Choi, H.Y. *Heat, Mass and Momentum Transfer*; Prentice Hall: Englewood Cliffs, NJ, 1963.

Received October 2001
Revised April 2002